Heliyon 9 (2023) e22533

Contents lists available at ScienceDirect

Heliyon

journal homepage: www.cell.com/heliyon

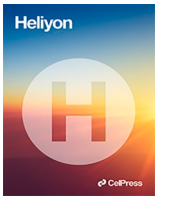

Growing crystals and studying structure and electronic properties of $Cu_2ZnGe(S_xSe_{1-x})_4$ compositions

Ivan V. Bodnar [a], Vitaly V. Khoroshko [a], Veronika A. Yashchuk [a], Valery F. Gremenok [a,b], Mohsin Kazi [c], Mayeen U. Khandaker [d,e], Abdul G. Abid [f,*], Tatiana I. Zubar [b], Daria I. Tishkevich [b], Alex V. Trukhanov [b,g,h], Sergei V. Trukhanov [b,g,**]

[a] Belarussian State University of Informatics and Radioelectronics, 220013, Minsk, P. Brovka str., 6, Belarus
[b] Laboratory of Magnetic Films Physics, SSPA "Scientific and Practical Materials Research Centre of NAS of Belarus", 220072, Minsk, P. Brovka str., 19, Belarus
[c] Department of Pharmaceutics, College of Pharmacy, POBOX-2457, King Saud University, Riyadh, 11451, Saudi Arabia
[d] Centre for Applied Physics and Radiation Technologies, School of Engineering and Technology, Sunway University, Bandar Sunway, 47500, Selangor, Malaysia
[e] Faculty of Graduate Studies, Daffodil International University, Daffodil Smart City, Birulia, Savar, Dhaka, 1216, Bangladesh
[f] Institute of Chemical Sciences, Bahauddin Zakariya University, Multan, 60800, Pakistan
[g] Smart Sensors Laboratory, Department of Electronic Materials Technology, National University of Science and Technology MISiS, Lenin Ave. 4/1, 119049, Moscow, Russia
[h] L.N. Gumilyov Eurasian National University, Astana, 010000, Kazakhstan

ARTICLE INFO

Keywords:
Single crystals
Chemical vapor transport method
Crystal structure
Microhardness
State diagram

ABSTRACT

Single crystals of $Cu_2ZnGeSe_4$ and Cu_2ZnGeS_4 solid solutions were developed and successfully obtained using the chemical vapor transfer method, with iodine acting as a transporter. The structure, compositional dependences of lattice parameters, pycnometric and X-ray densities and microhardness were determined. The chemical composition determined by the X-ray micro-analysis satisfactorily corresponds to the nominal one with a tolerance of ±5 %. The XRD analysis showed that all the obtained compounds and their solid solutions have unit cell described by tetragonal symmetry. The attice parameters were found to be $a = 5.342 \pm 0.005$ Å, $c = 10.51 \pm 0.01$ Å for the Cu_2ZnGeS_4 compound and $a = 5.607 \pm 0.005$ Å, $c = 11.04 \pm 0.01$ Å for the $Cu_2ZnGeSe_4$, respectively. Structural studies confirmed the validity of the Vegard's law in relation to the obtained samples. The pycnometric densities of ~4.28 g/cm^3 for the Cu_2ZnGeS_4 and ~5.46 g/cm^3 for the $Cu_2ZnGeSe_4$ were found to be slightly less than their X-ray densities of ~4.32 g/cm^3 and ~5.52 g/cm^3, respectively. The maximum microhardness of ~398 kg/mm^2 for these solid solutions corresponds to $x = 0.60$. The melt point of the solid solutions increases from ~1180 °C for the $Cu_2ZnGeSe_4$ up to ~1400 °C for the Cu_2ZnGeS_4. Based on X-ray fluorescence analysis and DTA data, the phase diagram of the $Cu_2ZnGeSe_4$-Cu_2ZnGeS_4 system was constructed. Analysis of the obtained diagram indicates its first type according to Rozbom's classification.

* Corresponding author.
** Corresponding author: s.v.trukhanov@gmail.com

https://doi.org/10.1016/j.heliyon.2023.e22533
Received 20 July 2023; Received in revised form 30 October 2023; Accepted 14 November 2023
Available online 18 November 2023

1. Introduction

The current level of consumption dictates an increased demand for the development and production of new materials with enhanced and improved physical and chemical properties [1–5]. Although composite materials are especially promising for technical and technological uses due to the combination of mechanical and electronic properties of different phases [6–10], pure compounds are still needed [11–13]. Very often pure compounds and their solid solutions in the form of single crystals are required in magnetic, microwave, optical and optoelectronic applications [14–16].

Single crystals have the highest degree of structural perfection compared to polycrystals and powders. The type and features of the structure together with the shape of the material, play an important role in the formation of electronic properties. Therefore, in optical and optoelectronic applications, the use of single crystals is preferable, since the influence of the near-surface layer is excluded.

These days particular attention is drawn to compounds with common formula $Cu_2A^{II}B^{IV}X_4^{VI}$, where A = Zn, Cd; B = Sn, Ge, Si and X = Te, Se, S. The study of such materials is a promising direction in semiconductor material science. These materials also include compounds Cu_2ZnGeS_4 and $Cu_2ZnGeSe_4$. The physical properties of films of the chalcogenides under consideration make it possible to use them as a plane-parallel absorbing layers in solar cells [17–20]. Although such materials are convenient for creation broadband photoconverters, receivers for near-infrared region of the spectrum, and other opto- and microelectronic devices, today the realization of the potential of these compounds encounters certain difficulties. The lack of reliable information about methods of obtaining, physico-chemical properties, and the connection of production technology for such crystals with their properties is main reason for impending progress of applied developments based on these materials. The growth of homogeneous in composition and properties single crystals of these compounds is a problem that has not been solved yet. In literature there is only fragmentary information on the growth of Cu_2ZnGeS_4, $Cu_2ZnGeSe_4$ crystals [21–26]. For solid solutions, information about their preparation and properties is even more scarce [27].

In present work the $Cu_2ZnGeSe_4$, Cu_2ZnGeS_4 compounds and their solid solutions were developed and successfully obtained using the chemical vapor transfer method, with iodine acting as a transporter, and their crystal structure and some mechanical properties were investigated. The chemical vapor transfer method is a practically significant method of atom-by-atom transfer, arrangement and growth of material, which allows the synthesis of highly perfect structures with well-controlled dimensions at sufficiently low temperatures and high purity.

2. Materials and methods

2.1. Singe crystals growth

Single crystals of Cu_2ZnGeS_4, $Cu_2ZnGeSe_4$ and $Cu_2ZnGeS_{4x}Se_{4(1-x)}$ solid solutions were grown from preliminary synthesized polycrystalline ingots by chemical vapor transport method in a vertical single-zone furnace. The diagram of the general organization of the developed methodology is presented in Fig. 1. The starting materials were copper, zinc, germanium, sulfur, and selenium with a purity >99.999 %. The required chemical components were taken in strict quantities of ~15–20 g and placed sequentially in two quartz ampoules, the inner one of which had a cone at one end. The pressure in the inner ampoule was fixed at the value of $\sim 10^{-3}$ Pa. A quartz rod attached to the bottom wall of the outer ampoule was a transmitter of vibrations from the vibrator. Vibratory mixing during synthesis can significantly accelerate the process of formation of the chemical phase of the sample and eliminate rupture of the ampoule.

At first, the furnace temperature increases up to 700–1000 K with a rate of ~50 K/h. At this stage, isothermal exposure with vibration was used for ~ 2–3 h. It was done to such volatile substances as sulfur and selenium managed to partially or completely reaction with cooper, zinc and germanium at this temperature and vapor pressure not more than 1 atm. Farther the temperature was increased up to ~1200–1400 K with the same rate and held for 2 h. The exact temperature in this range was depending on compound or solid solution composition being grown. Eventually, the vibration was eliminated and the directed crystallization of the melt occurred spontaneously under the influence of the cooling furnace down to ~1020–1080 K at a rate of ~100 K/h.

From the obtained polycrystalline ingots the required single crystals were grown using the chemical vapor transfer method with iodine acting as a transporter. The growth was realized in so called horizontal two-zone furnace. The single crystal growth process was completed in special quartz ampoules (d ~ 16–22 mm and L ~ 180 mm). Initially, the ampoule included two sections. Compounds Cu_2ZnGeS_4, $Cu_2ZnGeSe_4$ or $Cu_2ZnGeS_{4x}Se_{4(1-x)}$ solid solutions were loaded in form of a powder into one section, and a capillary with iodine, previously evacuated and soldered, was placeded into another. The transmitting agent concentration was ~5 mg/cm^3. The

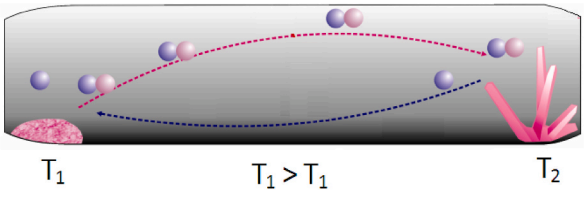

Fig. 1. Diagram of the general organization of the developed methodology. The pink balls are iodine atoms, while the purple balls are the transferred atoms of the growing single crystal.

pressure in the ampoule was ensured at a level of $\sim 10^{-3}$ Pa. After this, the capillary with iodine was uncorked with a "magnetic" hammer. Iodine was distilled into the section where ingots were located. The temperature in the reaction zone was maintained ~100 K lower than in the crystallization zone. This specific heating process was used to ensure that the reaction of the formation of metal iodides proceeded in a controlled manner and to remove possible uncontrolled crystallization centers. After exposure, the temperature in both zones equalized at 970–1070 K. The temperature gradient of ~70–100 K between the zones was finally established.

In these conditions, acicular, prismatic, and plate-like single crystals of Cu_2ZnGeS_4, $Cu_2ZnGeSe_4$ compounds and $Cu_2ZnGeS_{4x}Se_{4(1-x)}$ solid solutions were grown. They are shown in Figs. 2–5.

2.2. Investigation methods

The samples composition was determined by X-ray microanalysis using an electron microscope « Stereoscan-360». An « AVALON-8000» X-ray spectrometer was applied as an X-ray spectrum analyzer. Determination of the components had a tolerance of ±5 %.

The type of structure and lattice parameters of the grown samples were determined by X-ray diffraction (XRD) analysis. Diffraction patterns were fixed on a «DRON-3M » X-ray diffractometer, governed by a computer, in CuK_α-radiation and a nickel filter. The ground powder was pressed into a container to obtain a test sample, which were annealed in vacuum at a temperature of 650 K for ~2 h to relieve mechanical stress.

The method for determining pycnometric density is given in Ref. [28].

A microhardness tester "LEICA VMHT MOT" was used to determine the microhardness using the Knoop method. The (112) planes were used for plate-like single crystals for measurements. Hardness was calculated as the arithmetic mean over 20 points using the well-known formula [29].

The phase diagram of the resulting system was constructed based on the temperatures of phase transitions obtained using differential thermal analysis (DTA). The thermogram $\Delta T = f(T)$, where ΔT is the temperature difference between the test and standard samples, was fixed on specially designed equipment with an accuracy of ±2 K. The grounded powder was paced into Stepanov's quartz vessels. The vessels were pumped out down to the pressure of $\sim 10^{-3}$ Pa. Calcined alumina was applied as a standard. The temperature identity was reached by placing them in the sockets of a heat-resistant steel holder.

3. Results and discussion

The results of the X-ray microanalysis of the grown single crystals of Cu_2ZnGeS_4, $Cu_2ZnGeSe_4$ compounds and $Cu_2ZnGeS_{4x}Se_{4(1-x)}$ solid solutions are posted in Table 1. It can be seen that there is a slight deviation between the calculated and observed values.

The results of the XRD analysis showed that the diffraction patterns of Cu_2ZnGeS_4, $Cu_2ZnGeSe_4$ compounds and their solid solutions have reflection indices specific to tetragonal structure.

The lattice parameters for the Cu_2ZnGeS_4 compound are $a = 5.342 \pm 0.005$ Å, $c = 10{,}51 \pm 0.01$ Å, for $Cu_2ZnGeSe_4$ – $a = 5.607 \pm 0.005$ Å, $c = 11.04 \pm 0.01$ Å were calculated by the least square method. The change in these parameters with composition x is shown in Fig. 6.

It can be seen that the lattice parameters change linearly with the composition x, i.e. Vegard's law is fulfilled in the system under study and is described by the following relation (1):

$$a = 5.342 + 0.265x, c = 10.51 + 0.53x \quad (1)$$

The results of pycnometric density measurements of solid solution $Cu_2ZnGeS_{4x}Se_{4(1-x)}$ are presented in Fig. 6. It is shown that the density changes linearly with the composition x. The experimental lattice parameters were used for calculations of the X-ray density [30] using the following formula (2):

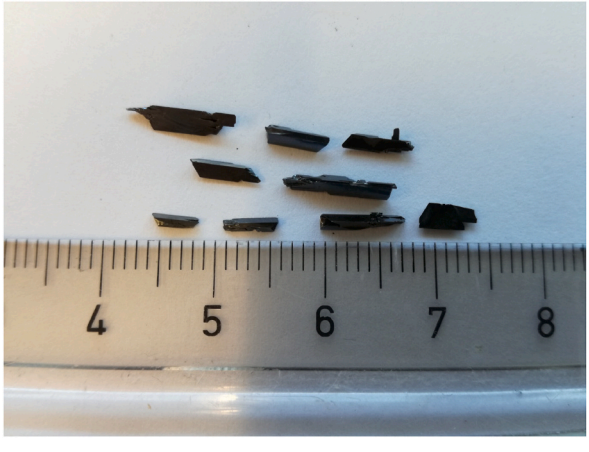

Fig. 2. Prismatic single crystals of Cu_2ZnGeS_4.

Fig. 3. Plate-lake single crystals $Cu_2ZnGeS_{2.0}Se_{2.0}$.

Fig. 4. Plate-lake single crystals $Cu_2ZnGeS_{2.8}Se_{1.2}$.

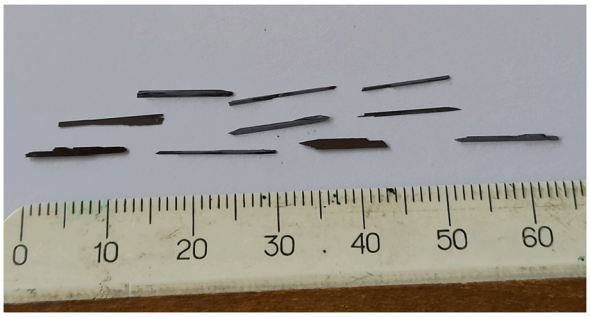

Fig. 5. Needle single crystals $Cu_2ZnGeSe_4$.

Table 1
The results of X-ray microanalysis of crystals of Cu_2ZnGeS_4, $Cu_2ZnGeSe_4$ compounds and $Cu_2ZnGeS_{4x}Se_{4(1-x)}$ solid solutions.

Compostion, *x*	Cu, at. %		Zn, at.%		Ge, at.%		S, at.%		Se, at.%	
	calc.	exp.	calc.	exp.	calc.	exp.	calc.	exp.	calc.	exp.
1.0	25.00	25.66	12.50	12.14	12.50	12.95	50.00	49.25	–	–
0.7	25.00	25.43	12.50	11.75	12.50	12.18	35.00	34.29	15.00	16.35
0.5	25.00	24.57	12.50	12.30	12.50	12.62	25.00	26.33	25.00	24.18
0.3	25.00	25.52	12.50	12.07	12.50	12.23	15.00	15.79	35.00	34.39
0.1	25.00	25.33	12.50	12.15	12.50	12.20	5.00	5.45	45.00	44.87
0.0	25.00	26.21	12.50	11.30	12.50	13.66	–	–	50.00	48.83

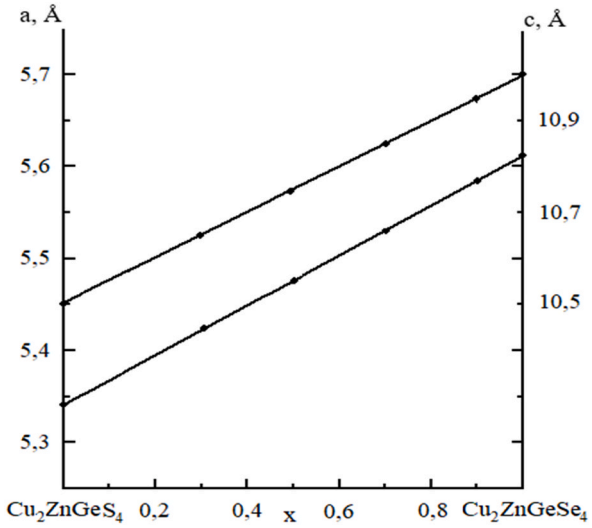

Fig. 6. Dependence of the unit cell parameters a and c on the composition x for $Cu_2ZnGeS_{4x}Se_{4(1-x)}$ solid solutions.

$$d_{x\text{-ray}} = 1,65 \bullet 10^{-24} \frac{n \bullet M}{V}, \tag{2}$$

where n is the atoms number in a unit cell; M is the molar mass of the sample; V is the volume of the unit cell, equal to $V = a^2c$.

The concentration dependence of the X-ray density is given in Fig. 7. The linearity in the change in both X-ray and pycnometric densities is clearly recorded. However, the X-ray density is slightly higher than the pycnometric density, which can be explained by the presence of structural defects in real crystals.

The experimental results of microhardness measurement are presented in Fig. 7. It is shown that the Kurankov's law is fulfilled to $Cu_2ZnGeS_{4x}Se_{4(1-x)}$ solid solutions. According to it, the concentration dependence of $H(x)$ is described by an upward smooth curve [31].

To describe this dependence, the following expression (3) was used [32]:

$$H = H_1 + (H_2 - H_1)x + (H_2 - H_1)\frac{1}{1-4\frac{M_1-M_2}{M_1+M_2}}x(1-x), \tag{3}$$

where H, H_1, H_2 are the values of microhardness of the solid solution and starter components, respectively; M_1 and M_2 are the molar masses of the starter components.

The calculated values of microhardness are shown in Fig. 8 by solid lines, experimental values are points. It can be seen that the experimental values are consistent with the calculated ones. The maximum on the curve $H = f(x)$ for these solid solutions corresponds to $x = 0.60$, i.e. the position of the maximum is shifted towards the Cu_2ZnGeS_4 compound with a higher microhardness.

The results of DTA are presented in Fig. 9. There is one thermal effect on the thermograms of both Cu_2ZnGeS_4 and $Cu_2ZnGeSe_4$ compounds and solid solutions based on them. It corresponds to the melt point of the compounds and to the solidus and liquidus points of the solid solutions.

According to the results of X-ray fluorescence analysis and DTA, a state diagram of the $Cu_2ZnGeSe_4$-Cu_2ZnGeS_4 system was plotted in Fig. 10. It can be seen that this state diagram is characterized by a relatively small crystallization interval and can be attributed to the first type according to Rosebom's classification.

When developing a technique for growing single crystals, it was necessary to solve the problem of optimizing the experimental conditions as a multifactorial problem with competing parameters [33–38]. Such problems are often encountered in the organization of experimental work [39–43] and the solution of multifactorial influences [44–49].

4. Conclusions

Single crystals of $Cu_2ZnGeSe_4$ and Cu_2ZnGeS_4 solid solutions were developed and successfully obtained using the chemical vapor transfer method, with iodine acting as a transporter. The composition of grown single crystals was determined by the X-ray microanalysis, and their structure and lattice parameters were determined by the XRD analysis. These parameters change with composition in accordance with Vegard's law. The pycnometric and X-ray densities, as well as microhardness, were determined. Their concentration dependences were plotted. The state diagram of the $Cu_2ZnGeSe_4$-Cu_2ZnGeS_4 system was plotted by X-ray fluorescence analysis and DTA. It can be attributed to the first type according to Rosebom's classification. The method used for growing single crystals of chalcogenides showed good results in the formation of structural perfection and, therefore, is recommended for obtaining similar

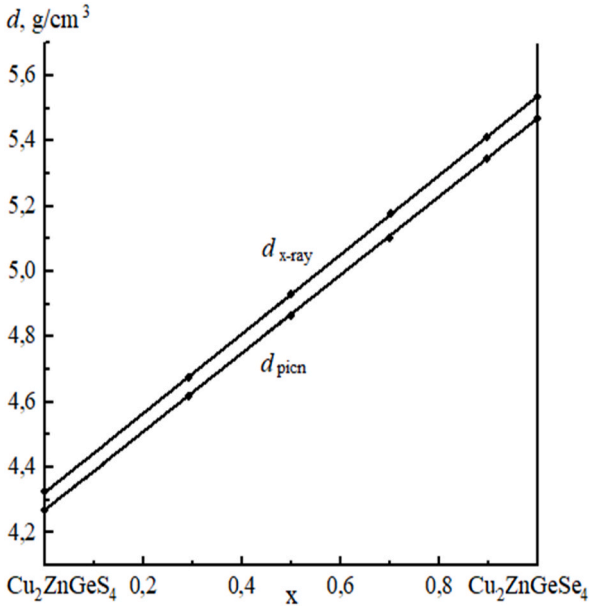

Fig. 7. Density change with composition x for $Cu_2ZnGeS_{4x}Se_{4(1-x)}$ solid solutions.

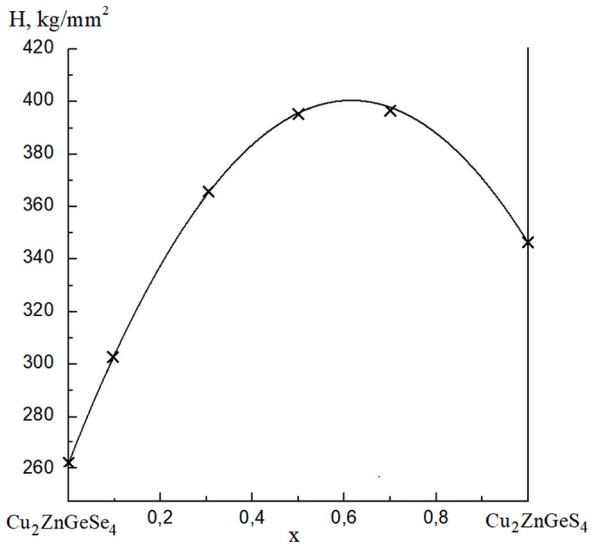

Fig. 8. Dependence of microhardness on composition x for $Cu_2ZnGeS_{4x}Se_{4(1-x)}$ solid solutions.

compounds.

Funding

This work was supported by the Belarusian State Programme for Research « Physical material science, new materials, and technologies» and partially by the European Project INFINITE-CELL (Ref. H2020-MSCA-RISE-2017-777,968, 2017–202100). The authors would like to extend their sincere appreciation to the Researchers Supporting Project Number (RSP2023R301), King Saud University, Riyadh, Saudi Arabia.

Institutional review board statement

Not applicable.

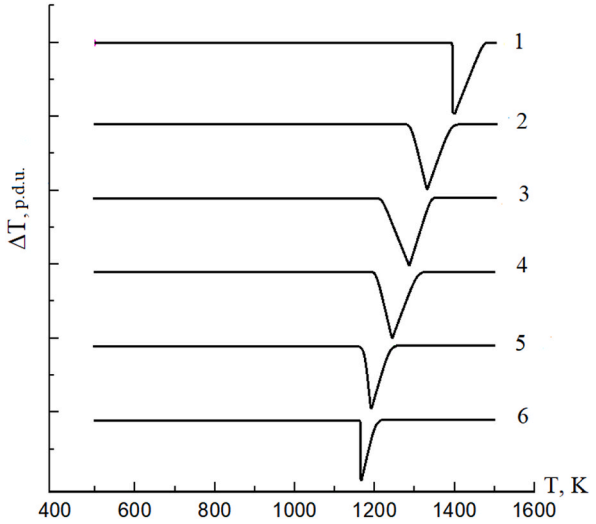

Fig. 9. Thermograms of $Cu_2ZnGeS_{4x}Se_{4(1-x)}$ crystals: 1 – x = 1.0; 2 – x = 0.7; 3 – x = 0.5; 4 – x = 0.3; 5 – x = 0.1; 6 – x = 0.0.

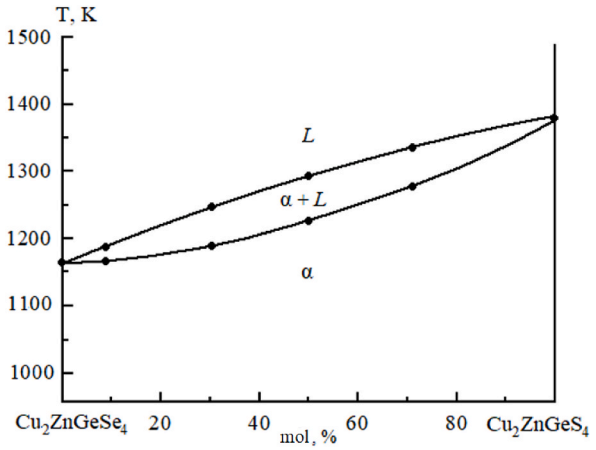

Fig. 10. The state diagram of the $Cu_2ZnGeSe_4$-Cu_2ZnGeS_4 system.

Informed consent statement

Not applicable.

Data availability statement

No data was used for the research described in the article.

CRediT authorship contribution statement

Ivan V. Bodnar: Writing – review & editing, Resources, Project administration, Funding acquisition, Formal analysis, Conceptualization. **Vitaly V. Khoroshko:** Writing – original draft, Visualization, Validation, Software, Resources, Methodology, Investigation, Data curation. **Veronika A. Yashchuk:** Writing – original draft, Visualization, Validation, Software, Methodology, Investigation, Data curation. **Valery F. Gremenok:** Writing – original draft, Supervision, Resources, Project administration, Formal analysis. **Mohsin Kazi:** Writing – review & editing, Resources, Project administration, Funding acquisition, Formal analysis. **Mayeen U. Khandaker:** Writing – review & editing, Supervision, Resources, Project administration, Funding acquisition, Formal analysis. **Abdul G. Abid:** Writing – original draft, Supervision, Software, Project administration, Investigation, Funding acquisition, Formal analysis. **Tatiana I. Zubar:** Writing – original draft, Visualization, Validation, Supervision, Software, Resources, Project administration, Investigation, Data curation. **Daria I. Tishkevich:** Writing – original draft, Visualization, Validation, Software, Resources, Project administration,

Funding acquisition, Data curation. **Alex V. Trukhanov:** Writing – review & editing, Writing – original draft, Supervision, Project administration, Investigation, Funding acquisition, Formal analysis, Data curation, Conceptualization. **Sergei V. Trukhanov:** Writing – review & editing, Writing – original draft, Supervision, Resources, Project administration, Investigation, Funding acquisition, Formal analysis, Data curation, Conceptualization.

Declaration of competing interest

The authors declare that they have no known competing financial interests or personal relationships that could have appeared to influence the work reported in this paper.

Acknowledgements

This work was supported by the Belarusian State Programme for Research « Physical material science, new materials, and technologies» and partially by the European Project INFINITE-CELL (Ref. H2020-MSCA-RISE-2017-777968, 2017–202100). The authors would like to extend their sincere appreciation to the Researchers Supporting Project Number (RSP2023R301), King Saud University, Riyadh, Saudi Arabia.

References

[1] A.R. Mahmood, M.A. Alheety, M.M.M. Asker, A.Z. Tareq, A. Karadağ, Saccharine based carbonyl multi-walled carbon nanotubes: novel modification, characterization and its ability for removing Cd(II) and Cu(II) from soil and environmental water samples, J. Phys: Conf. Ser. 1294 (2019), 052003, https://doi.org/10.1088/1742-6596/1294/5/052003.

[2] D.S.M. Subhi, L.I. Khaleel, M.A. Alheety, Preparation, characterization and H_2 storage capacity of newly Mn(II), Co(II), Ni(II), Cu(II) and Zn(II) mixed ligand complexes of paracetamol and saccharine, AIP Conf. Proc. 2213 (2020), 020306, https://doi.org/10.1063/5.0000077.

[3] B.D. Salih, A.H. Dalaf, M.A. Alheety, W.M. Rashed, I.Q. Abdullah, Biological activity and laser efficacy of new Co (II), Ni (II), Cu (II), Mn (II) and Zn (II) complexes with phthalic anhydride, Mater. Today: Proceed. 43 (2021) 869–874, https://doi.org/10.1016/j.matpr.2020.07.083.

[4] S.A. Al-Jibori, L.A. Al-Doori, A.S.M. Al-Janabi, M.A. Alheety, C. Wagner, A. Karadag, Mercury(II) mixed ligand complexes of phosphines or amines with 2-cyanoamino thiophenolate ligands formed via monodeprotonation and carbon–sulfur bond cleavage of 2-aminobenzothiazole. X-ray crystal structures of [Hg(SC_6H_4NCN)(PPh_3)]$_2$ and [Hg(SC_6H_4NCN)($Ph_2PCH_2PPh_2$)]$_2$, Polyhedron 206 (2021), 115349, https://doi.org/10.1016/j.poly.2021.115349.

[5] N.F. Alheety, L.A. Mohammed, A.H. Majeed, A. Aydin, K.D. Ahmed, M.A. Alheety, M.A. Guma, S. Dohare, Antiproliferative and antimicrobial studies of novel organic-inorganic nanohybrids of ethyl 2-((5-methoxy-1H-benzo[d]imidazole-2-yl)thio)acetate (EMBIA) with TiO_2 and ZnO, J. Molec. Str. 1274 (2023), 134489, https://doi.org/10.1016/j.molstruc.2022.134489.

[6] T.O. Abreu, R.F. Abreu, F.F. do Carmo, W.V. de Sousa, O. de, H. Barros, J.E.V. de Morais, J.P.C. do Nascimento, M.A.S. da Silva, S. Trukhanov, A. Trukhanov, L. Panina, C. Singh, A.S.B. Sombra, A novel ceramic matrix composite based on $YNbO_4$-TiO_2 for microwave applications, Ceram. Int. 47 (2021) 15424–15432, https://doi.org/10.1016/j.ceramint.2021.02.108.

[7] D.O. Shpylka, I.V. Ovsiienko, T.A. Len, L.Yu Matzui, S.V. Trukhanov, A.V. Trukhanov, O.S. Yakovenko, The features of the magnetoresistance of carbon nanotubes modified with Fe, Ceram. Int. 48 (2022) 19789–19797, https://doi.org/10.1016/j.ceramint.2022.03.253.

[8] M.A. Darwish, T.I. Zubar, O.D. Kanafyev, D. Zhou, E.L. Trukhanova, S.V. Trukhanov, A.V. Trukhanov, A.M. Henaish, Combined effect of microstructure, surface energy, and adhesion force on the friction of PVA/ferrite spinel nanocomposites, Nanomaterials 12 (2022) 1998, https://doi.org/10.3390/nano12121998.

[9] M.A. Almessiere, Y. Slimani, N.A. Algarou, M.G. Vakhitov, D.S. Klygach, A. Baykal, T.I. Zubar, S.V. Trukhanov, A.V. Trukhanov, H. Attia, M. Sertkol, I.A. Auwal, Tuning the structure, magnetic and high frequency properties of Sc-doped $Sr_{0.5}Ba_{0.5}Sc_xFe_{12-x}O_{19}$/$NiFe_2O_4$ hard/soft nanocomposites, Adv. Electr. Mater. 8 (2022), 2101124, https://doi.org/10.1002/aelm.202101124.

[10] M.A. Almessiere, N.A. Algarou, Y. Slimani, A. Sadaqat, A. Baykal, A. Manikandan, S.V. Trukhanov, A.V. Trukhanov, I. Ercan, Investigation of exchange coupling and microwave properties of hard/soft ($SrNi_{0.02}Zr_{0.01}Fe_{11.96}O_{19}$)/($CoFe_2O_4$)$_x$ nanocomposites, Mater. Today Nano 18 (2022), 100186, https://doi.org/10.1016/j.mtnano.2022.100186.

[11] D. Li, D. Zhou, D. Wang, W. Zhao, Y. Guo, Z. Shi, T. Zhou, S.-K. Sun, C. Singh, S. Trukhanov, A.S.B. Sombra, Lead-free relaxor ferroelectric ceramics with ultrahigh energy storage densities via polymorphic polar nanoregions design, Small 19 (2023), 2206958, https://doi.org/10.1002/smll.202206958.

[12] V.E. Zhivulin, E.A. Trofimov, O.V. Zaitseva, D.P. Sherstyuk, N.A. Cherkasova, S.V. Taskaev, D.A. Vinnik, YuA. Alekhina, N.S. Perov, K.C.B. Naidu, H.I. Elsaeedy, M.U. Khandaker, D.I. Tishkevich, T.I. Zubar, A.V. Trukhanov, S.V. Trukhanov, Preparation, phase stability and magnetization behavior of high entropy hexaferrites, iScience 26 (2023), 107077, https://doi.org/10.1016/j.isci.2023.107077.

[13] R.E. El-Shater, H. El Shimy, S.A. Saafan, M.A. Darwish, D. Zhou, K.C.B. Naidu, M.U. Khandaker, Z. Mahmoud, A.V. Trukhanov, S.V. Trukhanov, F. Fakhry, Fabrication of doped ferrites and exploration of its structure and magnetic behavior, Mater. Adv. 4 (2023) 2794–2810, https://doi.org/10.1039/d3ma00105a.

[14] I.V. Bodnar, S.V. Trukhanov, Magnetic properties of $Fe_xMn_{1-x}In_2S_4$ alloy single crystals, Semicond 45 (2011) 1408–1413, https://doi.org/10.1134/S106378261111008X.

[15] S.V. Trukhanov, I.V. Bodnar, M.A. Zhafar, Magnetic and electrical properties of ($FeIn_2S_4$)$_{1-x}$($CuIn_5S_8$)x solid solutions, J. Magn. Magn Mater. 379 (2015) 22–27, https://doi.org/10.1016/j.jmmm.2014.10.120.

[16] I.V. Bodnar, M.A. Jaafar, S.A. Pauliukavets, S.V. Trukhanov, I.A. Victorov, Growth, optical, magnetic and electrical properties of $CuFe_{2.33}In_{9.67}S_{17.33}$ single crystal, Mater. Res. Express 2 (2015), 085901, https://doi.org/10.1088/2053-1591/2/8/085901.

[17] W. Wang, M.T. Winkler, O. Gunawan, T. Gokmen, T.K. Todorov, Yu Zhu, D.B. Mitzi, Device characteristics of CZTSSe thin-film solar cells with 12.6% efficiency, Adv. Energ. Mater. 4 (2014), 1301465, https://doi.org/10.1002/aenm.201301465.

[18] T.K. Todorov, J. Tang, S. Bag, O. Gunawan, T. Gokmen, Yu Zhu, D.B. Mitzi, Beyond 11% efficiency: characteristics of state-of-the-art $Cu_2ZnSn(S,Se)_4$ solar cells, Adv. Energ. Mater. 3 (2013) 34–38, https://doi.org/10.1002/aenm.201200348.

[19] I. Repins, C. Beall, N. Vora, C. DeHart, D. Kuciauskas, P. Dippo, B. To, J. Mann, W.-C. Hsu, A. Goodrich, R. Noufi, Co-evaporated $Cu_2ZnSnSe_4$ films and devices, Sol. Energy Mater. Solar. Cells. 101 (2012) 154–159, https://doi.org/10.1016/j.solmat.2012.01.008.

[20] G.M. Ford, Q. Guo, R. Agrawal, H.W. Hillhouse, Earth abundant element $Cu_2Zn(Sn_{1-x}Ge_x)S_4$ nanocrystals for tunable band gap solar cells: 6.8% efficient device fabrication, Chem. Mater. 23 (2011) 2626, https://doi.org/10.1021/cm2002836.

[21] C.-I. Lee, C.-D. Kim, Optical properties of undoped and Co^{2+}-doped $Cu_2ZnGeSe_4$ crystals, J. Kor. Phys. Soc. 37 (2000) 364–367.

[22] K.I. Nakazawa, Electrical and optical properties of stannite-type quaternary semiconductor thin films, Jpn. J. Appl. Phys. 27 (1988) 2094–2097, https://doi.org/10.1143/JJAP.27.2094.

[23] N. Nakayama, K. Ito, Sprayed films of stannite Cu_2ZnSnS_4, Appl. Surf. Sci. 92 (1996) 171–174, https://doi.org/10.1016/0169-4332(95)00225-1.

[24] O.V. Parasyuk, L.D. Gulay, YaE. Romanyuk, L.V. Piskach, Phase diagram of the Cu_2GeSe_3 –ZnSe system and crystal structure of the $Cu_2ZnGeSe_4$ compound, J. Alloys Compd. 329 (2001) 202–207, https://doi.org/10.1016/S0925-8388(01)01606-1.

[25] M. León, S. Levcenko, R. Serna, G. Gurieva, A. Nateprov, J.M. Merino, E.J. Friedrich, U. Fillat, S. Schorr, E. Arushanov, Optical constants of Cu_2ZnGeS_4 bulk crystals, J. Appl. Phys. 108 (2010), 093502, https://doi.org/10.1063/1.3500439.

[26] S. Levcenco, M. Guc, C. Merschjann, G. Gurieva, S. Schorr, M. Lux-Steiner, E. Arushanov, Photoluminescence characterization of Cu2ZnGeS4 single crystals, Phys. Stat. Sol. 10 (2013) 1079–1081, https://doi.org/10.1002/pssc.201200843.

[27] E. Garcia-Llamas, J.M. Merino, R. Serna, X. Fontané, I.A. Victorov, A. Pérez-Rodríguez, M. León, I.V. Bodnar, V. Izquierdo-Roca, R. Caballero, Wide band-gap tuning $Cu_2ZnSn_{1-x}Ge_xS_4$ single crystals: optical and vibrational properties, Sol. Energy Mater. Solar Cells. 158 (2) (2016) 147–153, https://doi.org/10.1016/j.solmat.2015.12.021.

[28] G.A. Ilyinsky, Determination of the Density of Minerals, L.: Nedra, 1975, p. 119, p. (in Russian).

[29] V.M. Glazov, V.N. Vigdorovich, Microhardness of Metals and Semiconductors, M.: Metallurgy,, 1969, p. 248 (in Russian).

[30] S.S. Gorelik, IuA. Skakov, L.N. Rastorguev, X-Ray and Electron-Optical Analysis, MISIS Publ, Moscow, 1994, p. 366 (in Russian).

[31] N.S. Kurnakov, Introduction to Physical and Chemical Analysis, M.; L.: Publishing house of the Academy of Sciences of the USSR, 1940, p. 562 (in Russian).

[32] I.V. Bodnar, B.V. Korzun, A.P. Chernyakova, Microhardness of the $A^IB^{III}C_2^{VI}$ ternary semiconductors and their solid solutions, Phys. Stat. Sol. (a). 101 (1987) 409–419, https://doi.org/10.1002/pssa.2211010212.

[33] R. Rakkiyappan, A. Chandrasekar, J. Cao, Passivity and passification of memristor-based recurrent neural networks with additive time-varying delays, IEEE Trans. Neur. Netw. Learn. Syst. 26 (2015) 2043–2057, https://doi.org/10.1109/TNNLS.2014.2365059.

[34] A. Chandrasekar, R. Rakkiyappan, X. Li, Effects of bounded and unbounded leakage time-varying delays in memristor-based recurrent neural networks with different memductance functions, Neurocomp 202 (2016) 67–83, https://doi.org/10.1016/j.neucom.2016.04.012.

[35] A. Chandrasekar, T. Radhika, Q. Zhu, State estimation for genetic regulatory networks with two delay components by using second-order reciprocally convex approach, Neur. Proc. Lett. 54 (2022) 327–345, https://doi.org/10.1007/s11063-021-10633-4.

[36] A. Chandrasekar, T. Radhika, Q. Zhu, Further results on input-to-state stability of stochastic Cohen–Grossberg BAM neural networks with probabilistic time-varying delays, Neur. Proc. Lett. 54 (2022) 613–635, https://doi.org/10.1007/s11063-021-10649-w.

[37] M. Tamil Thendral, T.R. Ganesh Babu, A. Chandrasekar, Y. Cao, Synchronization of Markovian jump neural networks for sampled data control systems with additive delay components: analysis of image encryption technique, Math. Meth. Appl. Sci. (2022) 1–17, https://doi.org/10.1002/mma.8774.

[38] Radhika, T.; Chandrasekar, A.; Vijayakumar, V.; Zhu, Q. Analysis of Markovian jump stochastic Cohen–Grossberg BAM neural networks with time delays for exponential input-to-state stability. Neur. Proc. Lett. https://doi.org/10.1007/s11063-023-11364-4..

[39] A.Z. Tuleushev, F.E. Harrison, A.L. Kozlovskiy, M.V. Zdorovets, Evolution of the absorption edge of PET films irradiated with Kr ions after thermal annealing and ageing, Optical Mater 119 (2021), 111348, https://doi.org/10.1016/j.optmat.2021.111348.

[40] M.V. Zdorovets, A.L. Kozlovskiy, D.B. Borgekov, D.I. Shlimas, Influence of irradiation with heavy Kr^{15+} ions on the structural, optical and strength properties of BeO ceramic, J. Mater. Sci. Mater. Electron. 32 (2021) 15375–15385, https://doi.org/10.1007/s10854-021-06087-y.

[41] A.L. Kozlovskiy, A. Alina, M.V. Zdorovets, Study of the effect of ion irradiation on increasing the photocatalytic activity of WO_3 microparticles, J. Mater. Sci. Mater. Electron. 32 (2021) 3863–3877, https://doi.org/10.1007/s10854-020-05130-8.

[42] A.L. Kozlovskiy, M.V. Zdorovets, Study of hydrogenation processes in radiation-resistant nitride ceramics, J. Mater. Sci. Mater. Electron. 31 (2020) 11227–11237, https://doi.org/10.1007/s10854-020-03671-6.

[43] I.V. Korolkov, N. Zhumanazar, Y.G. Gorin, A.B. Yeszhanov, M.V. Zdorovets, Enhancement of electrochemical detection of Pb^{2+} by sensor based on track-etched membranes modified with interpolyelectrolyte complexes, J. Mater. Sci. Mater. Electron. 31 (2020) 20368–20377, https://doi.org/10.1007/s10854-020-04556-4.

[44] D.I. Shlimas, A.L. Kozlovskiy, M.V. Zdorovets, Study of the formation effect of the cubic phase of $LiTiO_2$ on the structural, optical, and mechanical properties of $Li_{2\pm x}Ti_{1\pm x}O_3$ ceramics with different contents of the *X* component, J. Mater. Sci.: Mater. Electron. 32 (2021) 7410–7422. https://doi.org/10.1007/s10854-021-05454-z.

[45] A.L. Kozlovskiy, D.I. Shlimas, M.V. Zdorovets, Synthesis, structural properties and shielding efficiency of glasses based on TeO_2-(1-x)ZnO-xSm_2O_3, J. Mater. Sci.: Mater. Electron. 32 (2021) 12111–12120. https://doi.org/10.1007/s10854-021-05839-0.

[46] A. Kozlovskiy, K. Egizbek, M.V. Zdorovets, M. Ibragimova, A. Shumskaya, A.A. Rogachev, Z.V. Ignatovich, K. Kadyrzhanov, Evaluation of the efficiency of detection and capture of manganese in aqueous solutions of $FeCeO_x$ nanocomposites doped with Nb_2O_5, Sensors 20 (2020) 4851. https://doi.org/10.3390/s20174851.

[47] M.V. Zdorovets, A.L. Kozlovskiy, D.I. Shlimas, D.B. Borgekov, Phase transformations in FeCo – Fe_2CoO_4/Co_3O_4-spinel nanostructures as a result of thermal annealing and their practical application, J. Mater. Sci.: Mater. Electron. 32 (2021) 16694–16705. https://doi.org/10.1007/s10854-021-06226-5.

[48] A.L. Kozlovskiy, M.V. Zdorovets, Synthesis, structural, strength and corrosion properties of thin films of the type CuX (X = Bi, Mg, Ni), J. Mater. Sci.: Mater. Electron. 30 (2019) 11819–11832. https://doi.org/10.1007/s10854-019-01556-x.

[49] I.Z. Zhumatayeva, I.E. Kenzhina, A.L. Kozlovskiy, M.V. Zdorovets, The study of the prospects for the use of $Li_{0.15}Sr_{0.85}TiO_3$ ceramics, J. Mater. Sci.: Mater. Electron. 31 (2020) 6764–6772. https://doi.org/10.1007/s10854-020-03234-9.